

Article

## Synthesis, Structure and Spectroscopy of Two Structurally Related Hydrogen Bonded Compounds in the *dpma*/HClO<sub>4</sub> System; *dpma* $\triangleq$ (dimethylphosphoryl)methanamine

Daniel Buhl, Hülya Gün, Alexander Jablonka and Guido J. Reiss \*

Institut für Anorganische Chemie und Strukturchemie, Lehrstuhl II: Material- und Strukturchemie, Heinrich-Heine-Universität Düsseldorf, Universitätsstraße 1, Düsseldorf D-40225, Germany; E-Mails: daniel.buhl@uni-duesseldorf.de (D.B.); huelya.guen@uni-duesseldorf.de (H.G.); alexander.jablonka@uni-duesseldorf.de (A.J.)

\* Author to whom correspondence should be addressed; E-Mail: reissg@hhu.de; Tel.: +49-211-81-13164; Fax: +49-211-81-14146.

Received: 17 February 2013; in revised form: 17 May 2013 / Accepted: 21 May 2013 /

Published: 5 June 2013

**Abstract:** The new phosphine oxide compound, (dimethylphosphoryl)methanaminium perchlorate, *dpma*HClO<sub>4</sub> (**1**), was synthesized by the reaction of (dimethylphosphoryl)methanamine (*dpma*) with concentrated perchloric acid. (Dimethylphosphoryl)methanaminium perchlorate (dimethylphosphoryl)methanamine solvate, *dpma*HClO<sub>4</sub>•*dpma* (**2**) was obtained by the slow evaporation of an equimolar methanolic solution of **1** and *dpma* at room temperature. For both compounds, single-crystal X-ray structures, IR and Raman spectra are reported. The assignment of the spectroscopic data were supported by quantum chemical calculations at the B3LYP/6-311G(2d,p) level of theory. In **1**, the *dpma*H cations form polymeric, polar double-strands along [010] by head to tail connections via N–H⋯O hydrogen bonds. The perchlorate anions are located between these strands attached by one medium strong and two weaker un-bifurcated hydrogen bonds (monoclinic, centrosymmetric space group *C2/c*, *a* = 17.8796(5) Å, *b* = 5.66867(14) Å, *c* = 17.0106(5) Å,  $\beta$  = 104.788(3)°, *V* = 1666.9(1) Å<sup>3</sup>, *Z* = 8, *T* = 293 K, *R*(*F*) [*I* > 2σ(*I*)] = 0.0391, *wR*(*F*<sup>2</sup>) [all] = 0.1113). In **2**, besides the N–H⋯O hydrogen bonds, medium strong N–H⋯N hydrogen bonds are present. One *dpma*H cation and the neutral *dpma* molecule are connected head to tail by two N–H⋯O hydrogen bonds forming a monocationic cyclic unit. These cyclic units are further connected by N–H⋯O and N–H⋯N hydrogen bonds forming polymeric, polar double-strands along [001]. The perchlorate anions fill the gaps between

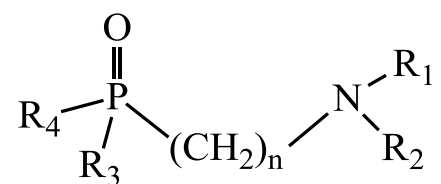
these strands, and each  $[\text{ClO}_4]^-$  anion is weakly connected to the  $\text{NH}_2$  group by one  $\text{N-H}\cdots\text{O}$  hydrogen bond (orthorhombic, non-centrosymmetric space group  $Pca2_1$  (No. 29),  $a = 18.5821(5) \text{ \AA}$ ,  $b = 11.4320(3) \text{ \AA}$ ,  $c = 6.89400(17) \text{ \AA}$ ,  $V = 1464.50(6) \text{ \AA}^3$ ,  $Z = 4$ ,  $T = 100 \text{ K}$ ,  $R(F) [I > 2\sigma(I)] = 0.0234$ ,  $wR(F^2) [\text{all}] = 0.0575$ ). Both structures are structurally related, and their commonalities are discussed in terms of a graph-set analysis.

**Keywords:** phosphine oxide; X-ray crystal structure; hydrogen bonding; graph-set analysis; tecton

## 1. Introduction

(Dialkylphosphoryl)alkanamines represent an interesting class of bidentate ligands (Scheme 1). Modification of the amino group is generally possible by a variation of the substituents,  $\text{R}_1$  and  $\text{R}_2$ . Alternatively, a change of the substituents at the phosphorous atom ( $\text{R}_3$  and  $\text{R}_4$ ) indirectly modifies the complex bonding properties of the oxygen atom of the phosphoryl group. Several  $\alpha$ -amino- $\omega$ -phosphine oxide alkanes with various chain lengths,  $n$ , and various substituents are structurally characterized [1–3]. A simple compound ( $n = 1$ ,  $\text{R}_1, \text{R}_2 = \text{H}$ ,  $\text{R}_3, \text{R}_4 = \text{CH}_3$ ) of this class is the (dimethylphosphoryl)methanamine (*dpma*). The synthesis of *dpma* has been reported more than twenty years ago [4,5], and also, the solid state structure of the *dpma* molecule has been determined [6]. There are structurally characterized examples for N-protonated salt structures (*dpmaHCl* [7], *dpmaH[MnCl\_3(H\_2O)\_2]* [8]), N-methylated cationic species [9] and more complex compounds [10]. It is also well known that *dpma* complexes of transition metals have been structurally characterized [6,11–13].

**Scheme 1.** General formula of a (dialkylphosphoryl)alkanamine.



Several fields of application of the above mentioned  $\alpha$ -amino- $\omega$ -phosphine oxide alkanes are reported. Tertiary phosphine oxides are useful for the formation and modification of phosphorus-containing polymers [14]. Recently, the synthesis and application of tunable phosphine oxide functionalized imidazolium ionic liquids has attracted much attention [15]. Moreover, tertiary phosphine oxides containing primary amine functionalization have been applied during the preparation of compounds with herbicidal properties [16,17]. Furthermore, these compounds show antitumor activity [12,18]. This contribution is part of our continuing interest of the hydrogen bonding architecture of phosphinic acid derivatives [7,8,19]. We here report on two new *dpmaH* salts in the *dpma/HClO\_4* system.

## 2. Results and Discussion

### 2.1. Structural Characterization of (Dimethylphosphoryl)methanaminium Perchlorate (**1**) and (Dimethylphosphoryl)methanaminium Perchlorate (Dimethylphosphoryl)methanamine Solvate (**2**)

Colorless block-shaped crystals of **1** have been obtained by the reaction of *dpma* with an excess of perchloric acid. The reaction of **1** with one equivalent of *dpma* and further recrystallization of the concluded crude product from methanol gave colorless plates of **2**. Details of crystal data and parameters for structure refinement of **1** and **2** are given in Table 1.

**Table 1.** Crystal data and parameters for structure refinement of **1** and **2**.

Compound	<b>1</b>	<b>2</b>
Empirical formula	C <sub>3</sub> H <sub>11</sub> NO <sub>5</sub> PCl	C <sub>6</sub> H <sub>21</sub> N <sub>2</sub> O <sub>6</sub> P <sub>2</sub> Cl
Formula weight (g mol <sup>-1</sup> )	207.55	314.64
Color	colorless	colorless
Habit	block	plate
Wavelength (Å)	0.71073	0.71073
Crystal system, space group	Monoclinic; C2/c (No. 15)	Orthorhombic; Pca2 <sub>1</sub> (No. 29)
Unit cell dimensions	<i>a</i> = 17.8796(5) Å	<i>a</i> = 18.5821(5) Å
	<i>b</i> = 5.66867(14) Å	<i>b</i> = 11.4320(3) Å
	<i>c</i> = 17.0106(5) Å	<i>c</i> = 6.8940(2) Å
	$\beta$ = 104.788(3) °	–
Volume (Å <sup>3</sup> )	1666.98(8)	1464.50(7)
<i>T</i> (K)	290	100
<i>Z</i>	8	4
Density (calcd.) (g cm <sup>-3</sup> )	1.654	1.427
Absorption coefficient (mm <sup>-1</sup> )	0.629	0.496
F(000)	864	664
Crystal size (mm <sup>3</sup> )	0.84 × 0.51 × 0.38	0.81 × 0.43 × 0.11
$\theta$ range for data collection (°)	2.95–30.00	3.56–29.99
Dataset (h; k; l)	–24:24; –7:7; –23:23	–25:26; –15:15; –9:9
Reflections collected	13,742	21,793
Independent reflections	2414	4198
Observed reflections [ <i>I</i> > 2 $\sigma$ ( <i>I</i> )]	2250	4050
Completeness (%)	99.9	99.3
Absorption correction	multi-scan	Gaussian
<i>T</i> <sub>min</sub> / <i>T</i> <sub>max</sub>	0.736/1.000	0.655/1.279
Refinement method	Least-squares matrix	Least-squares matrix
Data/restraints/parameters	2414/0/118	4198/1/187
Goodness-of-fit on F <sup>2</sup>	1.065	1.098
Final R indices [ <i>I</i> > 2 $\sigma$ ( <i>I</i> )]	<i>R</i> ( <i>F</i> ) = 0.0391; <i>wR</i> ( <i>F</i> <sup>2</sup> ) = 0.1085	<i>R</i> ( <i>F</i> ) = 0.0234; <i>wR</i> ( <i>F</i> <sup>2</sup> ) = 0.0575
R indices (all data)	<i>R</i> ( <i>F</i> ) = 0.0416; <i>wR</i> ( <i>F</i> <sup>2</sup> ) = 0.1113	<i>R</i> ( <i>F</i> ) = 0.0251; <i>wR</i> ( <i>F</i> <sup>2</sup> ) = 0.0585
( $\Delta$ / $\sigma$ ) <sub>max</sub>	0.000	0.001
$\Delta\rho_{\text{max}}/\Delta\rho_{\text{min}}$ (e Å <sup>-3</sup> )	1.456 */–0.292	0.276/–0.293
Flack parameter	–	0.66(4)
CCDC No.	922,354	922,355

\* All tested crystals show systematic non-merohedral twinning by metrical specialization (see Experimental section).

*dpma*HClO<sub>4</sub> (**1**) crystallizes in the centrosymmetric space group, *C2/c*, with one *dpma*H cation and one perchlorate anion in the asymmetric unit. All bond lengths and angles of the *dpma*H cation and the perchlorate anion are in the expected range (Tables 2 and 3). The crystal structure of **1** forms strands along the crystallographic *b*-axis (Figure 1). These strands are built by two polymeric hydrogen bonded chain structures, each consisting of *dpma*H cations connected head to tail ( $H_2 \cdots O_1' = 2.04(2)$  Å). The connection between these symmetry-dependent, parallel chains is realized by weaker hydrogen bonds ( $H_1 \cdots O_1'' = 2.30(3)$  Å) [20]. As a result of this structural motif, annealed nine-membered hydrogen bonded rings are obtained, which may be classified by a second level graph-set descriptor,  $R_3^2(9)$  [21–23]. The first level graph-set descriptor of the backbone of the chains is  $C_1^1(5)$ . Each *dpma*H cation forms only one moderate hydrogen bond [20] to the slightly distorted perchlorate anion (Tables 3 and 4). The principles of this structure are visualized by a so-called constructor graph [23] (Figure 1; right part). Figure 2 shows the packing diagram of the cationic strands and the  $[ClO_4]^-$  counter anion in the structure of **1**. As a consequence of the centrosymmetric space group symmetry, one half of the polar strands are aligned along and the other half opposite to the *b* direction (Figure 2).

**Table 2.** Selected atom distances [Å] in **1**.

Atoms	Distance	Atoms	Distance
P(1)–O(1)	1.4943(11)	P(1)–C(1)	1.8228(17)
P(1)–C(2)	1.7761(18)	N(1)–C(1)	1.474(2)
P(1)–C(3)	1.7795(16)	Cl(1)–O(11)	1.4334(15)
Cl(1)–O(12)	1.4239(16)	Cl(1)–O(13)	1.4306(15)
Cl(1)–O(14)	1.4389(15)	–	–

**Table 3.** Selected bond angles [°] in **1**.

Atoms	Angle	Atoms	Angle
O(1)–P(1)–C(2)	114.05(8)	O(1)–P(1)–C(3)	112.54(8)
O(1)–P(1)–C(1)	111.87(7)	C(1)–P(1)–C(2)	102.88(8)
C(2)–P(1)–C(3)	108.01(10)	N(1)–C(1)–P(1)	114.74(11)
C(1)–P(1)–C(3)	106.82(8)	O(11)–Cl(1)–O(12)	108.40(12)
O(11)–Cl(1)–O(13)	109.48(11)	O(11)–Cl(1)–O(14)	109.39(11)
O(12)–Cl(1)–O(13)	109.60(11)	O(12)–Cl(1)–O(14)	110.21(10)
O(13)–Cl(1)–O(14)	109.74(9)	O(1)–P(1)–C(1)–N(1)	–46.84(14)
C(2)–P(1)–C(1)–N(1)	–169.68(13)	C(3)–P(1)–C(1)–N(1)	76.71(14)

**Table 4.** Hydrogen bond parameters [Å and °] in **1**.

<i>d</i> (D–H⋯A)	<i>d</i> (D–H)	<i>d</i> (H⋯A)	<i>D</i> (D–H⋯A)	∠(DHA)
N1–H1⋯O1''	0.80(3)	2.30(3)	2.855(2)	127(3)
N1–H2⋯O1'	0.85(2)	2.04(2)	2.822(2)	151(2)
N1–H3⋯O11	0.92(3)	2.18(3)	3.032(2)	154(3)

Symmetry transformations used to generate equivalent atoms: ' =  $x - 1, -1 + y, z$ ; '' =  $0.5 - x, -0.5 + y, 0.5 - z$ .

**Figure 1.** Left part: hydrogen-bonding connection of the cations and anions of **1** via N–H···O hydrogen bonds forming strands along *b*. Blue numbers (1–9) indicate the second level graph-set  $R_3^2(9)$ ; the blue numbers (1–3) plus the red numbers (4–5) indicate the first level graph-set  $C_1^1(5)$ . The hydrogen bonds are shown by dashed lines. Primed atoms are related to those unprimed by the symmetry operations: ' =  $x - 1, -1 + y, z$ ; " =  $0.5 - x, -0.5 + y, 0.5 - z$ ; "' =  $0.5 - x, 0.5 + y, 0.5 - z$ . The displacement ellipsoids are drawn at the 50% probability level. Right part: constructor-graph of the part of the structure of **1** shown on the left side.

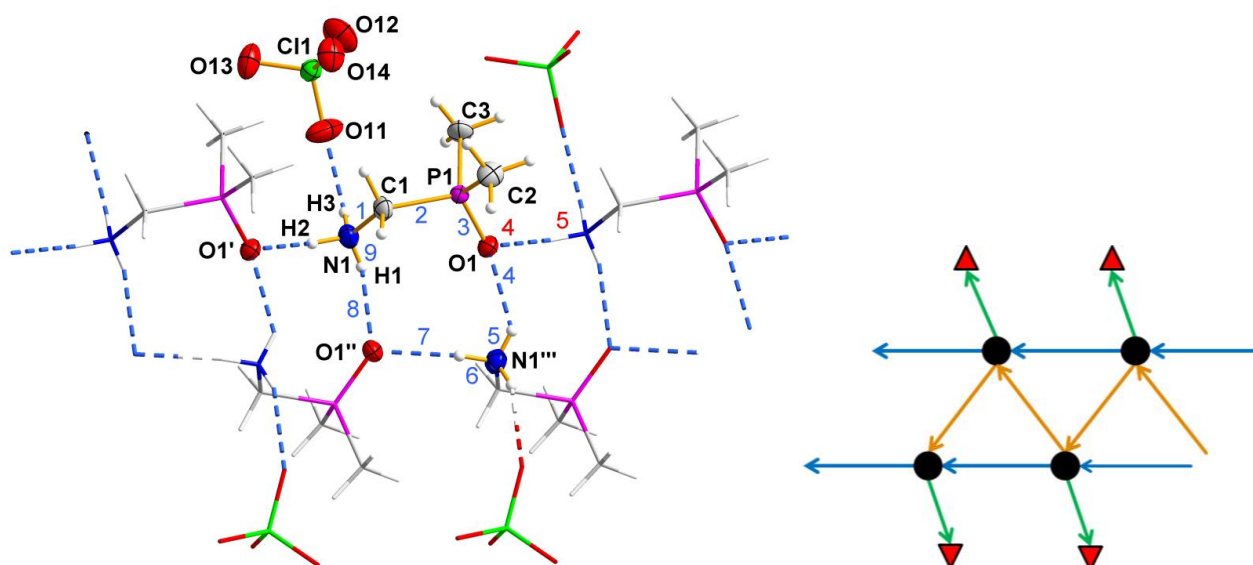
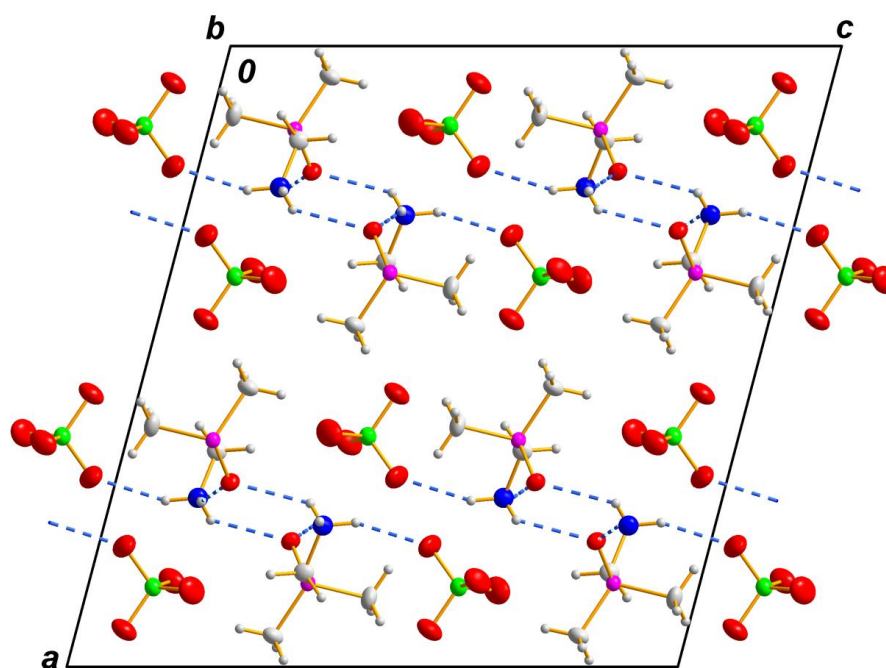


**Figure 2.** Packing diagram of **1** with view along  $[010]$ . Dashed lines are indicating N–H···O hydrogen bonds.



*dpmaHClO<sub>4</sub>·dpma* (**2**) crystallizes in the non-centrosymmetric space group, *Pca*2<sub>1</sub>. As illustrated in Figure 3, the asymmetric unit of **2** consists of one *dpmaH* cation, one *dpma* molecule and one nearly undistorted perchlorate anion. Bond lengths and angles within the *dpmaH* cation and in the neutral *dpma* molecule are as expected (Tables 5 and 6). The *dpmaH* cation and the *dpma* molecule are connected via a strong and a moderate N–H···O hydrogen bond (Table 7) to form a ten-membered ring (second level graph-set descriptor: R<sub>2</sub><sup>2</sup>(10); Figure 3 (blue numbers)).

**Figure 3.** Asymmetric unit of **2** (displacement ellipsoids drawn at the 50% probability level; blue numbers (1–10) indicate the second level graph-set, R<sub>2</sub><sup>2</sup>(10); symmetry codes: ' = *x*, *y*, 1 + *z*; " = 0.5 − *x*, *y*, 0.5 + *z*).

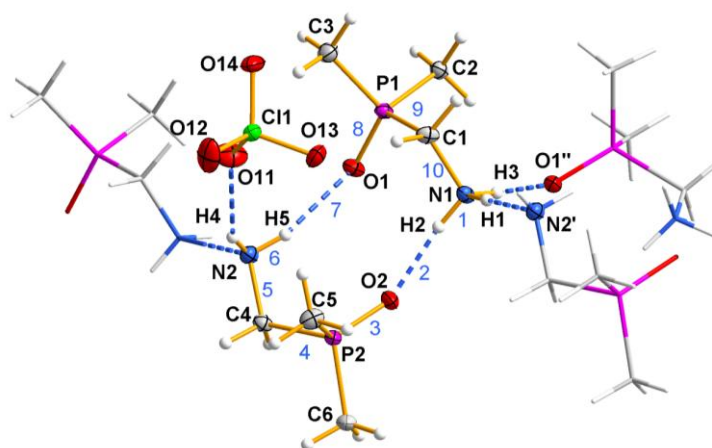


**Table 5.** Selected atom distances [Å] in **2**.

Atoms	Distance	Atoms	Distance
N(1)–C(1)	1.4831(18)	C(1)–P(1)	1.8249(14)
P(1)–O(1)	1.4989(10)	P(1)–C(2)	1.7875(13)
P(1)–C(3)	1.7830(14)	N(2)–C(4)	1.4725(18)
C(4)–P(2)	1.8127(14)	P(2)–O(2)	1.4987(10)
P(2)–C(5)	1.7877(15)	P(2)–C(6)	1.7911(13)
Cl(1)–O(11)	1.4359(12)	Cl(1)–O(12)	1.4303(11)
Cl(1)–O(13)	1.4378(11)	Cl(1)–O(14)	1.4374(11)

**Table 6.** Selected bond angles [°] in **2**.

Atoms	Angle	Atoms	Angle
N(1)–C(1)–P(1)	113.46(9)	O(1)–P(1)–C(1)	111.00(6)
O(1)–P(1)–C(2)	111.98(6)	O(1)–P(1)–C(3)	114.50(7)
C(1)–P(1)–C(2)	107.97(7)	C(1)–P(1)–C(3)	104.01(7)
C(2)–P(1)–C(3)	106.89(7)	N(2)–C(4)–P(2)	113.83(9)
O(2)–P(2)–C(4)	110.88(7)	O(2)–P(2)–C(5)	112.84(7)
O(2)–P(2)–C(6)	112.79(6)	C(4)–P(2)–C(5)	107.71(7)
C(4)–P(2)–C(6)	106.03(7)	C(5)–P(2)–C(6)	106.19(7)
O(11)–Cl(1)–O(12)	109.13(9)	O(11)–Cl(1)–O(13)	109.57(8)
O(11)–Cl(1)–O(14)	108.80(7)	O(13)–Cl(1)–O(14)	109.48(7)
O(12)–Cl(1)–O(13)	109.82(8)	O(12)–Cl(1)–O(14)	110.02(8)
N(1)–C(1)–P(1)–O(1)	42.01(12)	N(1)–C(1)–P(1)–C(2)	−81.07(11)
N(1)–C(1)–P(1)–C(3)	165.63(10)	N(2)–C(4)–P(2)–C(3)	−172.96(10)
N(2)–C(4)–P(2)–O(2)	−50.21(11)	N(2)–C(4)–P(2)–C(5)	73.70(11)

**Table 7.** Hydrogen bonds [ $\text{\AA}$  and  $^\circ$ ] in **2**.

D–H $\cdots$ A	d (D–H)	d (H $\cdots$ A)	d (D–H $\cdots$ A)	$\angle$ (DHA)
N1–H1 $\cdots$ N2'	0.89(2)	1.92(2)	2.8079(16)	178.4(18)
N1–H2 $\cdots$ O2	0.89(2)	1.838(19)	2.7173(15)	170.2(18)
N1–H3 $\cdots$ O1''	0.956(18)	1.853(19)	2.8069(16)	175.1(17)
N2–H4 $\cdots$ O11	0.827(18)	2.327(18)	3.0776(18)	151.3(17)
N2–H5 $\cdots$ O1	0.87(2)	2.17(2)	3.0015(16)	159.3(19)

Symmetry codes: ' =  $x, y, 1 + z$ ; '' =  $0.5 - x, y, 0.5 + z$ .

These cyclic units are furthermore connected head to tail to the units right and left by N–H $\cdots$ N hydrogen bonds giving a chain substructure (Figure 4, second level graph-set:  $C_2^2(7)$ ). Similarly to the structure of **1**, these chains are connected to a symmetry-related, hydrogen bonded chain by N–H $\cdots$ O hydrogen bonds constructing a strand. The connections of the *dpmaH*•*dpma* cyclic units within the strands furthermore produce one more simple ring-motif (Figure 4, black numbers), which can be described as a third level graph-set,  $R_4^3(11)$ . The strands in **2** run along [001]. The perchlorate anion forms only one weak hydrogen bond [20] to the amino group of the *dpma* molecule (Table 7). Furthermore, for this structure, the principles are visualized by a constructor graph [23] (Figure 4; right part). As illustrated in Figure 5 in the structure of **2**, the cationic part of the strands roughly form a hexagonal packing. Selected bond lengths and angles for (**2**) are listed in Tables 5 and 6. The relevant hydrogen bond parameters are presented in Table 7.

**Figure 4.** Showing *dpmaH*•*dpma* cyclic units (highlighted by a gray and a black arrow) and their crosslinks to form a complex one dimensional, hydrogen bonded strand (black numbers (1–11) indicate the third level graph-set,  $R_4^3(11)$ ).

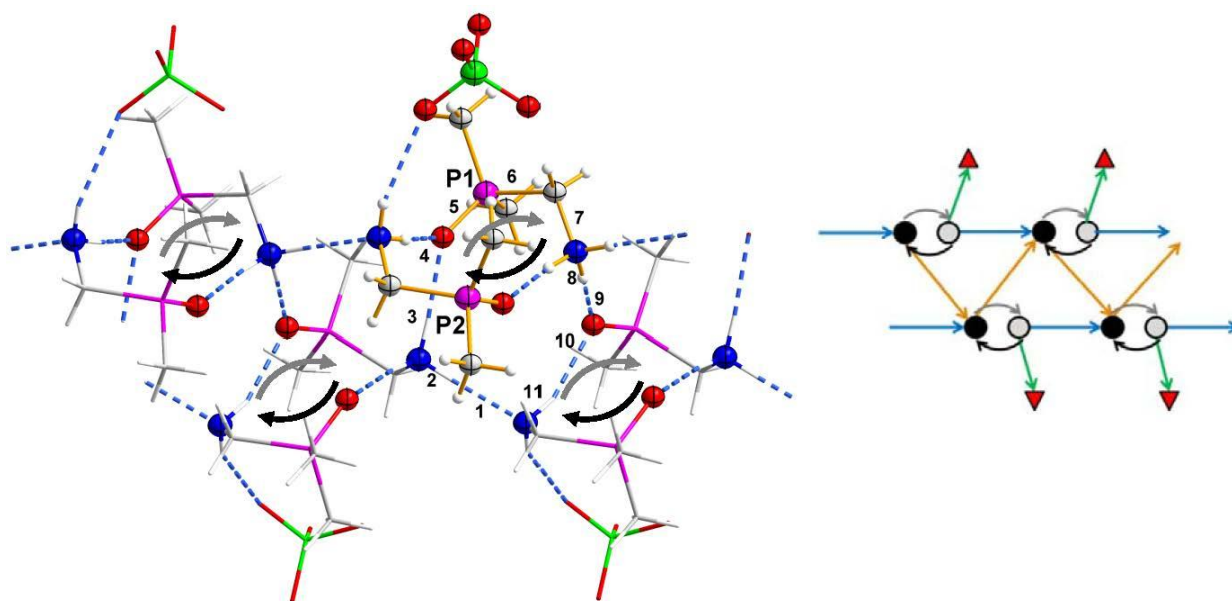
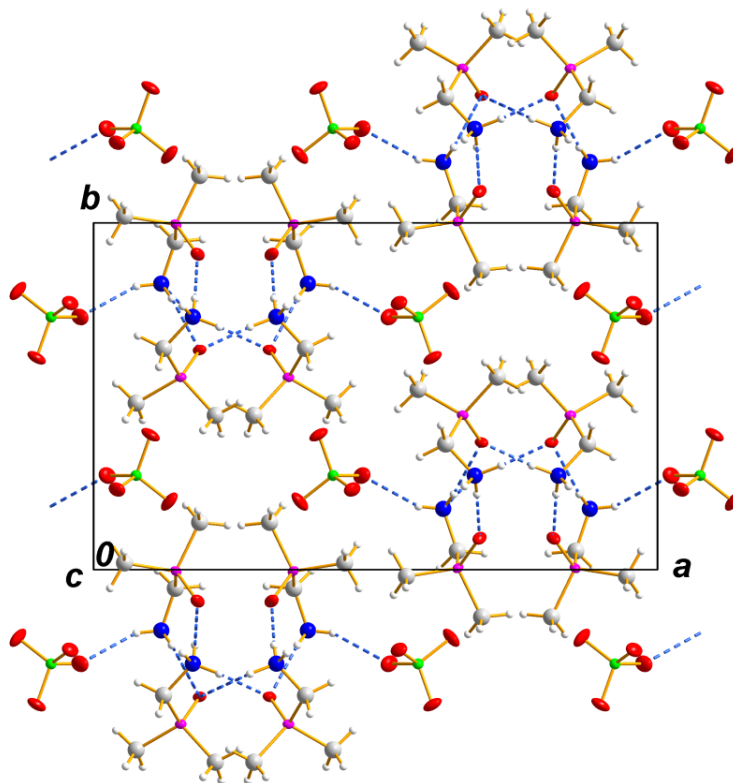


**Figure 5.** Packing diagram of (2), viewing direction [001]. Dashed lines are indicating N–H···O and N–H···N hydrogen bond contacts.



## 2.2. Vibrational Assignments of **1** and **2**

Compounds **1** and **2** were characterized by IR and Raman spectroscopy. The vibrational frequencies and their assignments are listed in Table S1 of the Supplementary Material. These assignments are based on calculated frequencies (B3LYP/6-311G(2d,p)). All over, the calculated frequencies are in good agreement with the experimental values, except the N-H stretching modes of the NH<sub>2</sub> and NH<sub>3</sub> moieties, respectively, which is a result of the involvement of the hydrogen atoms of the NH<sub>2</sub> and the NH<sub>3</sub> groups in hydrogen bonds in the solid state. Moreover, our assignments are in good agreement with known values in the literature [24]. The typical bands [25] for a slightly distorted perchlorate anion are present.

## 3. Experimental Section

### 3.1. Materials and Methods

All standard chemicals were used as purchased, whereas (dimethylphosphoryl)methanamine is accessible by a known synthesis in the literature [4,5]. Powder X-ray diffraction data of **1** and **2** were collected using a Stoe Stadi P diffractometer equipped with a linear position sensitive detector in transmission geometry and CuK $\alpha_1$  radiation. Diffraction data for phase identification was typically collected with a 0.1° step size. Structure refinements were performed using the derivative difference minimization (DDM) method. [26] The melting point of **1** was determined by means of the differential scanning calorimetry (DSC) method using a Mettler DSC 30 instrument. The sample was heated from

room temperature to 180 °C in nitrogen atmosphere with a heating rate of 5.0 °C/min. IR measurements were recorded on a Digilab Excalibur FTS 3500 spectrometer equipped with a single reflection ATR crystal. All IR spectra were collected over the range of 520–4000 cm<sup>-1</sup> with a resolution of 4 cm<sup>-1</sup>. Raman spectra were acquired at 8 cm<sup>-1</sup> (**1**) and 4 cm<sup>-1</sup> (*dpma*, **2**) spectral resolution over the range of 80–4000 cm<sup>-1</sup> using a MultiRam spectrometer (Bruker Optik, Ettlingen, Germany) (Nd:YAG-laser at 1064 nm; InGaAs-detector).

### 3.2. General Procedure for the Synthesis of **1** and **2**

(Dimethylphosphoryl)methanamine (0.12 g, 1.12 mmol) was dissolved in concentrated perchloric acid (1 mL, 30%). The colorless solution was heated to approximately 50 °C for a few minutes producing an oily bright yellow solution. Slow cooling to room temperature yielded colorless block-shaped crystals of (**1**) within three days. To purify (**1**), the excess solvent was removed *in vacuo* (0.20 g, 0.96 mmol, 86%). DSC (5.0 °C/min): T<sub>m</sub> = 162 °C, Δ<sub>m</sub>H = 8.453 kJ/mol.

An equimolar amount of (dimethylphosphoryl)methanamine (0.08 g, 0.77 mmol) was added to 0.16 g of (**1**) (0.77 mmol). After recrystallization from methanol (2.5 mL), the solution was dried in a vacuum desiccator obtaining (**2**) as colorless plates (0.14 g, 0.44 mmol, 57%).

### 3.3. X-ray Data Collection and Refinement

Crystallographic data collection for both compounds (**1**) and (**2**) was carried out using an Oxford-Xcalibur diffractometer equipped with monochromic MoKα radiation (λ = 0.71073 Å) and an EOS-CCD detector. The crystal data of **1** was measured at room temperature and that of **2** at 100 K. Absorption corrections were undertaken for both compounds (Table 1). Both structures were solved by applying direct methods with SHELXS-97 and refined against F<sup>2</sup> using all data by full-matrix least-squares techniques with SHELXL-97 [27]. Non-hydrogen atoms were refined using the anisotropic model. All hydrogen atoms in both structures were located from successive difference Fourier synthesis. In the final stages of the refinement of the structural model for the hydrogen atoms, a mixture of restrained and unrestrained parameters were used. Positional parameters of hydrogen atoms of the NH<sub>3</sub><sup>+</sup> and NH<sub>2</sub> group were refined freely in both structures.

Data collection of **1** was complicated by the fact that all tested crystals are uniquely non-merohedrally twinned (180° rotation along (100) in the reciprocal lattice; twin matrix: 1, -0.07, 0.053, 0, -1, 0, 0, 0, -1). The best results—concerning the plausibility of the structural model—were obtained for a crystal with only a small twin component. Here, the twin integration procedure cannot successfully integrate the reflections of the second twin component, because many of these weak reflections are very narrow to the strong reflections of the main component. To check the metric of the lattice, we collected powder diffraction data from the bulk material and re-refined the structure of **1** using the DDM method (*a* = 17.8802(7) Å, *b* = 5.6680(2) Å, *c* = 17.0357(6) Å, β = 104.711(2)°, R<sub>DDM</sub> 9.61, R<sub>Bragg</sub> = 12.71). The results are in excellent agreement with the lattice parameters and the space group assignment derived from the diffraction experiment using the twinned crystal. As a side effect, we were able to show that the bulk material is of high purity (Figure S1 of the Supplementary Material). We are convinced that the structural model is not affected by the twinning problem. A visible consequence of

this twinning phenomenon is an unusual high difference electron density of  $1.456 \text{ e}/\text{\AA}^3$  and a  $wR^2$  value, which is slightly higher than expected for this kind of compound (Table 1).

The measured crystal of **2** obviously was found to be an inversion twin. In the latest stages of the refinement, the ratio of the twin components were determined using the TWIN and BASF command of the SHELX System [27]; an approximate ratio of 2:1 (BASF 0.67(4)) for the two twin components was attained. Furthermore, in this case, a powder diffraction study and a structure refinement using the DDM-method on these data verified metrical parameter ( $a = 18.8049(5) \text{ \AA}$ ,  $b = 11.5653(3) \text{ \AA}$ ,  $c = 6.9391(1) \text{ \AA}$ ,  $R_{\text{DDM}} 8.84$ ,  $R_{\text{Bragg}} = 14.61$ ), space group and purity (Figure S2 of the Supplementary Material). All illustrated images of the molecular structures were created by using graphic program DIAMOND, a software for crystal and molecular structure visualization [28].

### 3.4. Computational Methods

The optimized geometry and vibrational frequencies of *dpma* were calculated at the density functional theory level by use of the B3LYP method, as implemented in the program *Gaussian 03* [29]. The 6-311G(2d,p) basis set was used. Calculations were performed on the GAUSS-Cluster at the Heinrich-Heine-Universität, Düsseldorf. The geometry of *dpma* has been confirmed by frequency analysis to be a minimum of the corresponding potential energy surface. The vibrational mode descriptions given in Table S1 of the Supplementary Material were assigned with the aid of *GaussView 3.0* [30].

## 4. Conclusions

This study shows the ability of the *dpmaH* tecton to form interesting hydrogen bonded architectures. In detail, the *dpmaH* tecton has a strong tendency to catenate to polar hydrogen bonded chains, which has been shown recently [7]. The head to tail connection of a neutral *dpma* molecule and a *dpmaH* cation gives a new tecton with just the same functionality as the simple cationic *dpmaH* tecton. As a consequence of this similarity of the building units, the hydrogen bonded structures of **1** and **2** are closely related. This relation is visualized by constructor graphs that focus on the most important features of these hydrogen bonded polymers.

## Acknowledgments

We thank E. Hammes and P. Roloff for technical support. We acknowledge the support for the publication fee by the Deutsche Forschungsgemeinschaft (DFG) and the open access publication fund of the Heinrich-Heine-Universität, Düsseldorf. Computational support and infrastructure was provided by the “Center for Information and Media Technology” (ZIM) at the Heinrich-Heine-Universität, Düsseldorf (Germany).

## Conflict of Interest

The authors declare no conflict of interest.

## References

1. Zagraniarsky, Y.; Ivanova, B.; Nikolova, K.; Varbanov, S.; Cholakova, T.Z. Synthesis of dimethylphosphinyl-substituted  $\alpha$ -Amino(aryl)methylphosphonic acids and their esters. *Naturforsch. B* **2008**, *63*, 1192–1198.
2. Rahman, M.S.; Steed, J.W.; Hii, K.K. Scope and Limitations of the Preparation of aminophosphines R-NH(CH<sub>2</sub>CH<sub>2</sub>PPh<sub>2</sub>) and aminodiphosphines R-N(CH<sub>2</sub>CH<sub>2</sub>PPh<sub>2</sub>)<sub>2</sub> via Michael addition of amines to vinylphosphines. *Synthesis* **2000**, *2000*, 1320–1326.
3. Ahmed, R.; Altieri, A.; D'Souza, D.M.; Leigh, D.A.; Mullen, K.M.; Pappmeyer, M.; Slawin, A.M.Z.; Wong, J.K.Y.; Woollins, J.D. Phosphorus-based functional groups as hydrogen bonding templates for rotaxane formation. *J. Am. Chem. Soc.* **2011**, *133*, 12304–12310.
4. Tsvetkov, E.N.; Kron, T.E.; Kabachnik, M.I. Synthesis of chloromethylphosphine oxides. *Izv. Akad. Nauk. Ser. Khim.* **1980**, *3*, 669–672.
5. Varbanov, S.G.; Agopian, G.; Borisov, G. Polyurethane foams based on dimethylaminomethylphosphine oxides adducts with ethylene and propylene oxides. *Eur. Polym. J.* **1987**, *23*, 639–642.
6. Kochel, A. Synthesis and magnetic properties of the copper(II) complex derived from dimethylaminomethylphosphine oxide ligand. X-ray crystal structure of DMAO and [Cu(NO<sub>3</sub>)<sub>2</sub>(POC<sub>3</sub>H<sub>10</sub>N)<sub>2</sub>]. *Inorg. Chim. Acta* **2009**, *362*, 1379–1382.
7. Reiss, G.J.; Jürgens, S. (Dimethylphosphoryl)methanaminium chloride. *Acta Cryst. E* **2012**, *68*, 2899–2900.
8. Reiss, G. Pseudosymmetric fac-diaquatrchlorido[(dimethylphosphoryl)methanaminium- $\kappa$ O]manganese(II). *Acta Cryst. E* **2013**, *69*, m250–m251.
9. Kaukorat, T.; Neda, I.; Jones, P.G.; Schmutzler, R. Formation of sulfenamides and sulfonamides bearing the organo-aminomethylene-dimethyl phosphine oxide or sulfide group. *Phosphorus Sulfur Silicon Relat. Elem.* **1997**, *122*, 33–47.
10. Varbanov, S.G.; Georgieva, A.; Hägele, G.; Keck, H.; Lachkov, V. Schiff bases derived from aminomethyl-dimethyl-phosphine oxide. *Phosphorus Sulfur Silicon Relat. Elem.* **2000**, *159*, 109–121.
11. Borisov, G.; Varbanov, S.G.; Venanzi, L.M.; Albinati, A.; Demartin, F. Coordination of dimethyl(aminomethyl)phosphine oxide with Zinc(II), Nickel(II), and Palladium(II). *Inorg. Chem.* **1994**, *33*, 5430–5437.
12. Dodoff, N.; Macicek, J.; Angelova, O.; Varbanov, S.G.; Spassovska, N. Chromium(III), Cobalt(II), Nickel(II) and Copper(II) complexes of (dimethylphosphinyl)methanamine. Crystal structure of fac-tris{(dimethylphosphinyl)methanamine-N, O}Nickel(II) chloride trihydrate. *J. Coord. Chem.* **1990**, *22*, 219–228.
13. Trendafilova, N.; Georgieva, I.; Bauer, G.; Varbanov, S.G.; Dodoff, N. IR and Raman study of Pt(II) and Pd(II) complexes of amino substituted phosphine oxides: Normal coordinate analysis. *Spectrochim. Acta A* **1997**, *53*, 819–828.

14. Klee, J.; Hörhold, H.; Schütz, H.; Varbanov, S.G.; Borisov, G. Unvernetzte epoxid-amin-additionspolymere, 21. dimethyl(aminomethyl)phosphinoxid, ein comonomeres für epoxidpolymere mit verminderter Entflammbarkeit (German). *Angew. Makromol. Chem.* **1989**, *170*, 145–157.
15. Vicente, J.A.; Mlonka, A.; Gunaratne, H.Q.N.; Swadźba-Kwaśny, M.; Nockemann, P. Phosphine oxide functionalized imidazolium ionic liquids as tuneable ligand for lanthanide complexation. *Chem. Commun.* **2012**, *48*, 6115–6117.
16. Maier, L. Organic phosphorus compounds 100 synthesis and properties of N-hydroxycarbonylmethyl-aminomethyl-dialkylphosphine oxides. *Phosphorus Sulfur Silicon Relat. Elem.* **1991**, *63*, 237–241.
17. Maier, L. Organic phosphorus compounds 93. Preparation, properties and herbicidal activity of 2-substituted 5-phenoxy- and 5-pyridyloxy-phenylaminoalkylphosphonic- and -phosphinic acid-as well as-phosphine oxide derivatives. *Phosphorus Sulfur Silicon Relat. Elem.* **1991**, *56*, 5–15.
18. Dodoff, N.; Varbanov, S.G.; Borisov, G.; Spassovska, N. Platinum(II), Platinum(IV), and Palladium(II) complexes of amino substituted phosphine oxides: Synthesis, characterization, and antitumor activity. *J. Inorg. Biochem.* **1990**, *39*, 201–208.
19. Meyer, M.K.; Graf, J.; Reiss, G.J. Dimer oder nicht dimer, das ist hier die Frage: Zwei benachbarte  $I_3^-$ -Ionen eingeschlossen in Hohlräumen einer komplexen Wirtsstruktur (German). *Z. Naturforsch. B* **2010**, *65*, 1462–1466.
20. Jeffrey, G.A. *An Introduction to Hydrogen Bonding*; Oxford University Press: New York, NY, USA, 1997; p. 12.
21. Bernstein, J.; Davis, R.E.; Shimon, L.; Chang, N. Patterns in hydrogen bonding: Functionality and graph set analysis in crystals. *Angew. Chem. Int. Ed.* **1995**, *34*, 1555–1573.
22. Etter, M.C.; MacDonald, J.C.; Bernstein, J. Graph-Set analysis of hydrogen-bond patterns in organic crystals. *Acta Cryst.* **1990**, *B46*, 256–262.
23. Grell, J.; Bernstein, J.; Tinhofer, G. Graph-set analysis of hydrogen-bond patterns: Some mathematical concepts. *Acta Cryst.* **1999**, *B55*, 1030–1043.
24. Kolev, T.M.; Varbanov, S.G.; Stamboliyska, B.A.; Hägele, G.; Russeva, E.D. Experimental and computational studies of the structure and vibrational spectra of aminomethyl-dimethyl-phosphine oxide and its  $^{15}N$  labeled isomer. *Spectrochim. Acta A* **2004**, *60*, 2993–3000.
25. Nakamoto, K. *Infrared and Raman Spectra of Inorganic and Coordination Compounds Part A: Theory and Applications in Inorganic Chemistry*; John Wiley & Sons, Inc.: New York, NY, USA, 1997; p. 199.
26. Solovyov, L.A. Full-profile refinement by derivative difference minimization. *J. Appl. Crystallogr.* **2004**, *37*, 743–749.
27. Sheldrick, G.M. A short history of SHELX. *Acta Cryst. A* **2008**, *64*, 112–122.
28. Brandenburg, K. *Diamond*; Crystal Impact GbR: Bonn, Germany, 2011.

29. Frisch, M.J.; Trucks, G.W.; Schlegel, H.B.; Scuseria, G.E.; Robb, M.A.; Cheeseman, J.R.; Montgomery, J.J.A.; Vreven, T.; Kudin, K.N.; Burant, J.C.; Millam, J.M.; Iyengar, S.S.; Tomasi, J.; Barone, V.; Mennucci, B.; Cossi, M.; Scalmani, G.; Rega, N.; Petersson, G.A.; Nakatsuji, H.; Hada, M.; Ehara, M.; Toyota, K.; Fukuda, R.; Hasegawa, J.; Ishida, M.; Nakajima, T.; Honda, Y.; Kitao, O.; Nakai, H.; Klene, M.; Knox, J.E.; Li, X.; Hratchian, H.P.; Cross, J.B.; Bakken, V.; Adamo, C.; Jaramillo, J.; Gomperts, R.; Stratmann, R.E.; Yazyev, O.; Austin, A.J.; Cammi, R.; Pomelli, C.; Ochterski, J.W.; Ayala, P.Y.; Morokuma, K.; Voth, G.A.; Salvador, P.; Dannenberg, J.J.; Zakrzewski, V.G.; Dapprich, S.; Daniels, A.D.; Strain, M.C.; Farkas, O.; Malick, D.K.; Rabuck, A.D.; Raghavachari, K.; Foresman, J.B.; Ortiz, J.V.; Cui, Q.; Baboul, A.G.; Clifford, S.; Cioslowski, J.; Stefanov, B.B.; Liu, G.; Liashenko, A.; Piskorz, P.; Komaromi, I.; Martin, R.L.; Fox, D.J.; Keith, T.; Al-Laham, M.A.; Peng, C.Y.; Nanayakkara, A.; Challacombe, M.; Gill, P.M.W.; Johnson, B.; Chen, W.; Wong, M.W.; Gonzalez, C.; Pople, J.A. *Gaussian 03*; Gaussian, Inc.: Wallingford, CT, USA, 2004.
30. Dennington, R.I.; Keith, T.; Millam, J.M.; Eppinnett, K.; Hovell, W.L.; Gilliland, R. *GaussView 3.0*; Crystal Impact GbR: Bonn, Germany, 2003.

© 2013 by the authors; licensee MDPI, Basel, Switzerland. This article is an open access article distributed under the terms and conditions of the Creative Commons Attribution license (<http://creativecommons.org/licenses/by/3.0/>).